



AMERICAN METEOROLOGICAL SOCIETY

Monthly Weather Review

EARLY ONLINE RELEASE

This is a preliminary PDF of the author-produced manuscript that has been peer-reviewed and accepted for publication. Since it is being posted so soon after acceptance, it has not yet been copyedited, formatted, or processed by AMS Publications. This preliminary version of the manuscript may be downloaded, distributed, and cited, but please be aware that there will be visual differences and possibly some content differences between this version and the final published version.

The DOI for this manuscript is doi: 10.1175/MWR-D-12-00309.1

The final published version of this manuscript will replace the preliminary version at the above DOI once it is available.

If you would like to cite this EOR in a separate work, please use the following full citation:

Hamill, T., F. Yang, C. Cardinali, and S. Majumdar, 2013: Impact of Targeted Winter Storm Reconnaissance Dropwindsonde Data on Mid-latitude Numerical Weather Predictions. *Mon. Wea. Rev.* doi:10.1175/MWR-D-12-00309.1, in press.



1 **Impact of Targeted Winter Storm Reconnaissance Dropwindsonde Data**
2 **on Mid-latitude Numerical Weather Predictions**

3 Thomas M. Hamill¹, Fanglin Yang^{2,3}, Carla Cardinali⁴,
4 and Sharanya J. Majumdar⁵

5 ¹ *NOAA Earth System Research Lab, Physical Sciences Division, Boulder, Colorado*

6 ² *I.M. Systems Group, Inc., Rockville, Maryland*

7 ³ *NOAA/NCEP Environmental Modeling Center, College Park, Maryland*

8 ⁴ *European Centre for Medium Range Weather Forecasts, Reading, England*

9 ⁵ *Rosenstiel School of Marine and Atmospheric Science, University of Miami, Florida.*

10

11 Revised for *Monthly Weather Review* as an expedited contribution

12

4 December 2012

13

Corresponding author address:

14

Dr. Thomas M. Hamill

15

NOAA Earth System Research Lab, Physical Sciences Division

16

R/PSD1, 325 Broadway

17

Boulder, Colorado, USA 80305

18

tom.hamill@noaa.gov, (303) 497-3060

19
20
21
22
23
24
25
26
27
28
29
30
31
32
33
34
35
36
37
38
39
40
41

Abstract

The impact of assimilating data from the 2011 Winter Storm Reconnaissance (WSR) program on numerical weather forecasts was assessed. Parallel sets of analyses and deterministic 120-h numerical forecasts were generated using the ECMWF 4D-Var and Integrated Forecast System. One set of analyses was generated with all of the normally assimilated data plus WSR targeted dropwindsonde data, the other with only the normally assimilated data. Forecasts were then generated from the two analyses. The comparison covered the period from 10 January 2011 to 28 March 2011, during which 98 flights and 776 total dropwindsondes were deployed from four different air bases in the Pacific basin and US. The dropwindsondes were deployed in situations where guidance indicated the potential for high-impact weather and/or the potential for large subsequent forecast errors. Downstream target verification regions where the high-impact weather was expected were identified for each case. Forecast errors around the target verification regions were evaluated using an approximation to the total-energy norm. Precipitation forecasts were also evaluated over the contiguous US using the equitable threat score and bias.

Forecast impacts were generally neutral and thus smaller than reported in previous studies, most from over a decade ago, perhaps because of the improved forecast and assimilation system and the somewhat denser observation network. Target areas may also have been under-sampled in this study. The neutral results from 2011 suggest that it may be more beneficial to explore other targeted observation concepts for the mid-latitudes, such as assimilation of a denser set of cloud-drift winds and radiance data in dynamically sensitive regions.

42 1. Introduction

43 Since the mid-1990s, supplementary “targeted” atmospheric observations have
44 been deployed in relative data voids in the extratropics, such as the open ocean under
45 cloud shields. The additional data were collected in an attempt to improve the operational
46 numerical weather prediction (NWP) of potential high-impact weather events through
47 assimilation of these extra data. The most extensive use of targeted observations in the
48 extratropics has been through the annual National Oceanographic and Atmospheric
49 Administration (NOAA) Winter Storm Reconnaissance (WSR) program, which has been
50 operational since 2001. During each day of WSR, NOAA forecasters identify weather
51 systems that may impact the contiguous United States and Alaska up to a week in advance
52 and estimate the uncertainty associated with the forecast of each system. They pick a
53 “target verification location” where the high-impact weather is centered and then
54 subjectively assign a low, medium or high priority to each case depending on the severity of
55 the event and the potential impact to society. The Ensemble Transform Kalman Filter
56 technique (ETKF, Bishop et al. 2001) is then used to identify potential upstream “sensitive
57 areas,” primarily over the northern Pacific Ocean, in which the assimilation of targeted
58 observations is expected to maximally improve the subsequent forecast of the weather
59 event in question. More specifically, the ETKF uses wind and temperature output at the
60 200, 500 and 850 hPa pressure levels from operational ensemble forecasts generated at the
61 National Centers for Environmental Prediction (NCEP), the European Centre for Medium-
62 Range Weather Forecasts (ECMWF) and the Canadian Meteorological Centre (CMC).
63 Perturbations from these ensemble forecasts about their respective center’s ensemble
64 means are used to predict error covariance matrices, and thereby the reduction in forecast

65 error variance due to any potential deployment of targeted observations (for example, a
66 flight track). In other words, the variance of the “signal”, meaning the impact of the
67 targeted observations using a difference total energy metric, is predicted and mapped as a
68 composite ‘summary map’ that depict sensitive areas for sampling, and also as a function of
69 a pre-defined series of flight tracks (Majumdar et al. 2002a). Once the optimal flight tracks
70 have been determined by the ETKF for the aircraft that release the Global Positioning
71 System (GPS) dropwindsondes, a flight request is submitted two days prior to the actual
72 flight deployment. These data are then assimilated into operational global NWP systems.
73 For more comprehensive details of the field of targeted observations, the interested reader
74 is referred to review articles by Langland (2005) and Majumdar et al. (2011).

75 The decision to implement WSR in NOAA’s operations was based on the promising
76 results of the NORPEX-98 and experimental WSR field campaigns in 1999 and 2000, in
77 which verification studies found that the majority of lower-resolution targeted forecasts
78 were significantly improved (Langland et al. 1999; Szunyogh et al. 2000, 2002).
79 Additionally, evaluations of the ETKF had demonstrated that it can efficiently and
80 accurately predict the reduction in the error variance of 1-3 day forecasts due to targeted
81 observations, prior to each deployment (Majumdar et al. 2001, 2002a). The broader-scale
82 aspects of ETKF targets were largely found to agree with those of adjoint-based techniques
83 such as singular vectors (Majumdar et al. 2002b). Recent studies have demonstrated the
84 utility of the ETKF out to 7 days, with sensitive areas traceable as far upstream as Japan
85 (Sellwood et al. 2008; Majumdar et al. 2010). Consequently, WSR aircraft have been
86 stationed in Japan since 2009 to collect targeted observations, in an attempt to improve
87 medium-range forecasts.

88 Since the advent of WSR, much has changed in numerical weather prediction (NWP),
89 and there are concerns in the community that previous optimistic results from over a
90 decade ago may not be replicable today. Forecast models are now much higher in
91 resolution and incorporate better physical parameterizations, thus producing better prior
92 forecasts for the data assimilation. Additionally, advanced data assimilation methods such
93 as 4-dimensional variational assimilation (4D-Var) are now operational at almost all NWP
94 centers, reducing analysis errors further. The observing network is also more extensive
95 than it was a decade ago, as is the assimilation of satellite data in operational NWP systems.
96 Finally, there is concern that the areas that need to be sampled may be so prohibitively
97 large that ~10-20 additional dropwindsondes per flight may be inadequate (Langland
98 2005).

99 WSR has not recently performed careful data denial experiments with a modern
100 data assimilation and forecast system, testing the forecast impact with and without the
101 targeted observations. This paper reports on an attempt to perform such an experiment
102 using 2011 WSR data and the ECMWF assimilation and forecast system. The hypothesis to
103 be tested is as follows: given a reasonably selected set of targeted observations, forecasts
104 that incorporate the assimilation of these additional observations will be significantly more
105 skillful than forecasts that do not, and the extra observations will be especially important
106 for cases with anticipated high-impact weather, often associated with rapidly developing
107 cyclones and rapid growth of forecast error. Examples of cases in which large forecast
108 errors are associated with deepening cyclones are presented in Colle and Charles (2011).
109 Further, we hypothesize that the impact of the targeted observations will be larger in

110 specific downstream ‘verification regions’ focused on the expected area with high-impact
111 weather and that the impact will be smaller when evaluated over continental-sized areas.

112 **2. Targeted data, model, and data assimilation system**

113 The WSR program is coordinated each year by the NOAA National Centers for
114 Environmental Prediction (NCEP), who have kept a log of daily flight requests, and the
115 forecast lead time, verification time, target verification locations, and the priority of each
116 forecast case at http://www.nco.ncep.noaa.gov/pmb/sdm_wsr/ from 2003 to the present.

117 In 2011, a total of 776 dropwindsondes were deployed by the NOAA and USAF aircraft
118 which took off from four different air bases (Anchorage, Biloxi, Yokota Japan, and
119 Honolulu). During the 2011 WSR period there were 22 high-priority cases, 62 medium-
120 priority cases, and 14 low-priority cases. The forecast lead time associated with a given
121 target verification for an event ranged from +12 hours to +120 hours post assimilation.
122 The lead time was calculated as the difference between the forecast target verification time
123 and the initialization time. A plot of the target verification locations during the 2011 WSR
124 campaign from 10 January 2011 through 26 March 2011 is shown in Fig. 1, including the
125 assigned priority for each target and the forecast lead time.

126 Two parallel forecast experiments were carried out using the ECMWF’s 4D-Var data
127 assimilation system and global weather forecast model for the period from 9 January 2011
128 through 28 March 2011. The first set included the 2011 WSR dropwindsonde data
129 (“CONTROL”) and the second set excluded the dropwindsonde data (“NODROP”). For both
130 assimilation cycles, $\sim 10^7$ other observations were assimilated in both CONTROL and
131 NODROP experiments, i.e., the full data stream normally assimilated at ECMWF. In

132 particular, the surface-based observations were SYNOP (measuring surface pressure, 10-m
133 winds, and 2-m relative humidity), DRIBU (buoys measuring surface pressure and 10-m
134 winds), radiosonde (measuring temperature, winds, and humidity profiles), aircraft
135 (measuring temperature and wind profile), profilers, and PIBAL (measuring wind profiles).
136 From the geostationary platforms (Meteosat, GOES, MTSAT, and MODIS), two different
137 observation types were assimilated, atmospheric motion vectors (retrieved wind profiles)
138 and infrared sounder radiances. From the polar orbiting platforms, the following were
139 assimilated: AMSU-A, AMSU-B, MHS and MSG (all measuring microwave-sounder radiance),
140 IASI, AIRS and HIRS (measuring infrared-sounder radiance), SSMI, SSMIS, TMI, AMSR-E
141 (microwave-imager radiance), ASCAT and ERS (retrieved wind product from microwave
142 scatterometer backscatter coefficients), and GPS-Radio Occultation (measuring radio
143 occultation bending angle). Both CONTROL and NODROP were cycled continuously for the
144 entire campaign period, whether the targeted dropwindsonde data were available or not.
145 When targeted observations were taken, subsequent deterministic forecasts were
146 produced to +120 hours lead. In all cases, the CONTROL analysis was used for verification,
147 which may bias the results at the early leads slightly to favor the CONTROL forecasts. For
148 both cycles, ECMWF used version 37r2 of their Integrated Forecast System (IFS;
149 www.ecmwf.int/products/data/operational_system/evolution/evolution_2011.html). The
150 resolution of the forecast model was T511 (~0.35-degree grid spacing on reduced linear
151 Gaussian grid), with 91 vertical levels. The data assimilation, ECMWF's 4D-Var system,
152 uses a full nonlinear trajectory at T511 L91 (outer loop) and a linearized model (Janiskova
153 and Lopez 2012) at the resolutions T159, T159, and T255 for the three minimization inner
154 loops, respectively. The ECMWF 4D-Var system also used background error variances "of

155 the day” as estimated from the low resolution (T399 L91 outer loop, linearized T159 inner
 156 loops) ensemble data assimilation (Bonavita et al. 2010).

157 **3. Description of norms used to evaluate forecast impact.**

158 The impact of assimilating the dropwindsonde data on ECMWF forecast skill was
 159 calculated using a crude approximation to the commonly used dry total-energy norm. This
 160 norm is similar to the total-energy metric used in the ETKF computations of signal variance.
 161 Let \mathbf{u} represent a gridded state vector of forecast minus analysis differences for the u -wind
 162 component. Similarly, \mathbf{v} , \mathbf{t} , and \mathbf{p} represent fields of differences in v -wind, temperature, and
 163 surface pressure. Then the error E for a domain A was

$$164 \quad E = \left[\frac{1}{2} \int_A \left(\frac{1}{4} \left(\mathbf{u}_{250}^2 + \mathbf{v}_{250}^2 + \frac{c_p}{T_r} \mathbf{t}_{250}^2 \right) + \right. \right. \quad (4)$$

$$\left. \frac{1}{4} \left(\mathbf{u}_{500}^2 + \mathbf{v}_{500}^2 + \frac{c_p}{T_r} \mathbf{t}_{500}^2 \right) + \right. \quad (4)$$

$$\left. \frac{1}{4} \left(\mathbf{u}_{850}^2 + \mathbf{v}_{850}^2 + \frac{c_p}{T_r} \mathbf{t}_{850}^2 \right) + \right. \quad (4)$$

$$\left. \frac{1}{4} \left(\mathbf{u}_{10m}^2 + \mathbf{v}_{10m}^2 + \frac{c_p}{T_r} \mathbf{t}_{2m}^2 \right) + R_d T_r \left(\frac{\mathbf{p}}{P_r} \right)^2 \right]^{1/2}, \quad (4)$$

165 where the state vector subscripts denote the constant pressure level (250 hPa, 500 hPa,
 166 850 hPa) or the height above ground (10 m, 2 m). c_p represents the specific heat content of
 167 dry air at constant pressure ($= 1004 \text{ J K}^{-1} \text{ kg}^{-1}$), T_r is the reference temperature ($= 300\text{K}$),
 168 R_d is the gas constant for dry air ($= 287 \text{ J K}^{-1} \text{ kg}^{-1}$), and P_r is the reference pressure ($= 1000$
 169 hPa). The integral sign indicates that the error was integrated and averaged over the
 170 domain A , accounting for latitudinal variations in grid spacing. The domain A will differ

171 with different tests. This approximation to the total-energy norm provides a little extra
172 weight to near-surface fields, which may be desirable given their greater societal relevance.
173 The impact was first evaluated in relatively confined verification regions, +/- 10 degrees
174 latitude and longitude around the verification location of interest at the specific lead time
175 of the target forecast, which may change from +12 h to +120 h depending on the case day.
176 This size of verification region was chosen to closely resemble the 10-degree radius region
177 used in previous WSR evaluations. Next, similar statistics were computed within a larger
178 Pacific/North American (PNA) region covering North America and adjacent coastal waters
179 (20° N - 75° N, 180° E - 320° E). Equitable threat scores and bias (Wilks 2006, eqs. 7.18
180 and 7.10, respectively) were also computed over the contiguous United States (CONUS).
181 Precipitation forecasts were evaluated at stations, bilinearly interpolating the forecast data
182 to gauges within the CONUS that report 24-h accumulated amounts.

183 **4. Forecast impact.**

184 Figure 2 provides a comparison of the forecast errors for NODROP vs. CONTROL.
185 Panel (a) provides a scatterplot of the data, with the CONTROL errors on the abscissa and
186 NODROP errors on the ordinate. There is a symbol associated with each case, with
187 different symbols for the different lead times. Cases above the diagonal line indicate cases
188 with some improvement from the assimilation of dropwindsonde data. Panel (b) provides
189 another way of viewing the differences, this time as a scatterplot as a function of the
190 forecast lead time. Different symbols indicate the different priorities assigned to the cases.
191 The solid line provides the mean difference for each lead time, and the dashed line
192 indicates one standard deviation. While there are some slight positive differences, there

193 are about as many negative differences. This 2011 data do not support the hypothesis that
194 the differences with vs. without targeted observations are statistically significant in the
195 localized verification region. From visual inspection, there is no obvious relationship
196 between the priority of the case and the impact; in fact, the forecast impact of high-priority
197 cases appear well mixed with the ones of medium- and low-priority cases. Objective
198 statistics as a function of the priority were not calculated because of the small sample sizes.
199 Figure 3 provides the same type of information, but here over the PNA region. The forecast
200 errors averaged over this larger area are also very similar between CONTROL and NODROP.
201 A different forecast skill index such as the anomaly correlation (e.g, 500 hPa time series,
202 not shown) also showed a similar lack of impact.

203 We also examined the precipitation equitable threat scores and biases for both +24
204 to +48 h accumulations (Fig. 4) and for +48 to +72 h accumulations (Fig. 5) over the
205 contiguous US. The differences are not statistically significant.

206 **5. Discussions and conclusions.**

207 This study has briefly summarized the impact from the assimilation of targeted
208 observations from the 2011 Winter Storms Reconnaissance Program. Parallel cycles of
209 ECMWF's data assimilation and deterministic forecasts were conducted, including and
210 excluding the targeted observations with the rest of the regularly assimilated data.
211 Differences were not statistically significant. The 2011 results do not support the
212 hypothesis that differences between forecasts with and without these assimilated
213 dropwindsondes are statistically significantly improved in the localized verification region.
214 There may be several reasons for the lack of impact noted here. Observing systems have

215 gotten denser in the ~10 years since the last systematic, peer-reviewed studies including
216 the Pacific basin, with more cloud-track winds, aircraft, satellite radiance, and radio
217 occultation data from global positioning satellites. Many other observing systems may now
218 have relatively limited impact were they evaluated in a similar observing systems
219 experiment. Data assimilation and forecast systems have improved as well. Additionally, it
220 is recognized that a handful of dropwindsondes will incompletely sample the initial
221 sensitive area due to limitations on how far and where the plane deploying them can fly. It
222 is also worth recognizing that while the ETKF targeting technique has quantitatively
223 proven to be skillful in predicting signal variance for short-range forecasts of winter
224 weather, it is imperfect and also inconsistent with the operational data assimilation scheme
225 used in this study. One might expect the ETKF to be more effective if an ensemble-based
226 data assimilation scheme is used to assimilate the targeted data. However, it is generally
227 accepted (e.g. Majumdar et al. 2011) that the targeting method is not the first-order
228 problem.

229 It might be possible that data from different years or seasons has a different impact.
230 Recently, R. Gelaro (personal communication, 2012) found that using NASA's adjoint
231 sensitivity method and their assimilation system (Gelaro et al. 2010), the assimilated
232 dropwindsonde data had a large positive impact on a global measure of 24-h forecast error
233 in several cases during WSR 2012. However, these impact results have not yet been
234 measured with an observing system experiment such as were conducted here.

235 For the foreseeable future, the global observing network will continue to have
236 regions with relatively sparse in-situ data. The challenge will be to supplement the existing

237 network in the most cost-effective manner. WSR plane flights into the central Pacific are
238 typically quite expensive, with fuel costs alone typically in the tens of thousands of US
239 dollars. In a comparison study of observation impacts in three forecast systems, Gelaro et
240 al. (2010) showed that only a small majority of the total number of assimilated
241 observations actually improve the 24-h forecast, with much of the improvement coming
242 from a large number of observations having relatively small individual impacts. Those
243 authors argue that accounting for this behavior may be especially important when
244 considering strategies for deploying adaptive components of the observing system. Given
245 this and the results of the present study, we suggest refocusing the targeting concept to use
246 available resources such as high-resolution satellite data. Sensitive areas, whether they are
247 determined by forecasters or by objective algorithms, can potentially be monitored more
248 closely by turning on the rapid-scan feature on geostationary satellites and then
249 assimilating a denser network of motion vectors, such as in Berger et al. (2011). Perhaps a
250 denser network of radiance data can be assimilated in sensitive regions (Bauer et al. 2011).

251

252

253 **Acknowledgments:**

254 Members of the THORPEX Data Assimilation and Observing Systems Committee are
255 thanked for providing guidance on the experimental design and the methods for
256 verification and for informal reviews of this manuscript. Publication of this article was
257 supported with a grant from the NOAA THORPEX program, managed by John Cortinas,
258 director of the Office of Weather and Air Quality.

259

260 **References**

- 261 Bauer, P., R. Buizza, C. Cardinali, and J.-N. Thepaut, 2011: Impact of singular vector based
262 satellite data thinning on NWP. *Quart. J. Royal Meteor. Soc.*, **137**, 277-285.
- 263 Berger, H., R. H. Langland, C. S. Velden, C. A. Reynolds, and P. M. Pauley, 2011. Impact of
264 Enhanced Satellite-Derived Atmospheric Motion Vector Observations on Numerical
265 Tropical Cyclone Track Forecasts in the Western North Pacific during TPARC/TCS-
266 08. *J. Applied Meteor. Clim.*, **50**, 2309-2318.
- 267 Bishop, C. H., B. J. Etherton, and S. J. Majumdar, 2001: Adaptive sampling with the Ensemble
268 Transform Kalman Filter. Part I: Theoretical aspects. *Mon. Wea. Rev.*, **129**, 420-436.
- 269 Bonavita, M., L. Raynaud, and L. Isaksen, 2010: Estimating background error variances
270 with the ECMWF ensemble of data assimilation: the effect of ensemble size and day-
271 to-day variability. *Quart. J. Royal Meteor. Soc.*, **137**, 423-434.
- 272 Colle, B. A. and M. E. Charles, 2011: Spatial Distribution and Evolution of Extratropical
273 Cyclone Errors over North America and its Adjacent Oceans in the NCEP Global
274 Forecast System Model. *Wea. Forecasting*, **26**, 129-149.
- 275 Gelaro, R., R. H. Langland, S. Pellerin, and R. Todling, 2010: The THORPEX observation
276 impact intercomparison experiment. *Mon. Wea. Rev.*, **138**, 4009-4025.
- 277 Janiskova, M., and P. Lopez, 2012. Linearized physics for data assimilation at ECMWF.
278 ECMWF Technical Memorandum 666. Available at
279 <http://www.ecmwf.int/publications/library/do/references/show?id=90382>

280 Langland, R. H., Z. Toth, R. Gelaro, I. Szunyogh, M. A. Shapiro, S. Majumdar, R. Morss, G. D.
281 Rohaly, C. Velden, N. Bond, and C. Bishop, 1999: The North-Pacific Experiment
282 (NORPEX-98) Targeted observations for improved North American Weather
283 Forecasts. *Bull. Amer. Meteorol. Soc.*, **80**, 1363-1384.

284 Langland, R. H., 2005: Issues in targeted observing. *Quart. J. Royal Meteor. Soc.*, **131**, 3409-
285 3425.

286 Majumdar, S. J., C. H. Bishop, B. J. Etherton, I. Szunyogh and Z. Toth, 2001: Can an ensemble
287 transform Kalman filter predict the reduction in forecast-error variance produced
288 by targeted observations? *Quart. J. Royal Meteor. Soc.*, **127**, 2803–2820.

289 Majumdar, S. J., C. H. Bishop, B. J. Etherton and Z. Toth, 2002a: Adaptive sampling with the
290 ensemble transform Kalman filter. II: Field program implementation. *Mon. Wea. Rev.*,
291 **130**, 1356–1369.

292 Majumdar, S. J., C. H. Bishop, R. Buizza and R. Gelaro, 2002b: A comparison of ensemble-
293 transform Kalman-filter targeting guidance with ECMWF and NRL total-energy
294 singular vector guidance. *Q. J. R. Meteorol. Soc.*, **128**, 2527–2549.

295 Majumdar, S. J., K. J. Sellwood, D. Hodyss, Z. Toth and Y. Song, 2010: Characteristics of target
296 areas selected by the Ensemble Transform Kalman Filter for medium-range
297 forecasts of high-impact winter weather. *Mon. Wea. Rev.*, **138**, 2803-2824.

298 Majumdar, S. J., S. D. Aberson, C. H. Bishop, C. Cardinali, J. Caughey, A. Doerenbecher, P.
299 Gauthier, R. Gelaro, T. M. Hamill, R. H. Langland, A.C. Lorenc, T. Nakazawa, F. Rabier,
300 C. A. Reynolds, R. Saunders, Y. Song, Z. Toth, C. Velden, M. Weissmann, and C.-C. Wu,

301 2011: Targeted observations for improving numerical weather prediction: an
302 overview. World Weather Research Programme/THORPEX Publication No. 15, 37
303 pp. Available at
304 [http://www.wmo.int/pages/prog/arep/wwrp/new/documents/THORPEX No 15.](http://www.wmo.int/pages/prog/arep/wwrp/new/documents/THORPEX%20No%2015.pdf)
305 [pdf.](http://www.wmo.int/pages/prog/arep/wwrp/new/documents/THORPEX%20No%2015.pdf)

306 Sellwood, K. J., S. J. Majumdar, B. E. Mapes and I. Szunyogh, 2008: Predicting the influence of
307 observations on medium-range winter weather forecasts. *Quart. J. Roy. Meteor. Soc.*,
308 **134**, 2011-2027.

309 Szunyogh, I., Z. Toth, S. Majumdar, R. Morss, B. Etherton, and C. Bishop, 2000: The effect of
310 targeted dropwindsonde observations during the 1999 Winter Storm
311 Reconnaissance program. *Mon. Wea. Rev.*, **128**, 3520-3537.

312 Szunyogh, I., Toth, Z., Zimin, A. V., Majumdar, S. J. and Persson, A. 2002: Propagation of the
313 effect of targeted observations: The 2000 Winter Storm Reconnaissance Program.
314 *Mon. Wea. Rev.*, **130**, 1144–1165.

315 Wilks, D. S., 2006: *Statistical Methods in the Atmospheric Sciences*. Academic Press, 627 pp.
316

317 **Figure captions.**

318 **Figure 1:** Scatterplot of the target central locations. Triangles denote low-priority cases,
319 filled circles for medium-priority, squares for high priority. The forecast lead time is
320 denoted by the color of the symbol, indicated by the legend on the left-hand side.

321 **Figure 2.** (a) Scatterplot of forecast errors for the target verification regions, CONTROL (x-
322 axis) vs. NODROP (y-axis). Data for the different forecast lead times are denoted by
323 different symbols, as shown in the figure legend. (b) Differences of RMS errors in the
324 energy norm between the NODROP and CONTROL experiments. Bold line indicates the
325 mean difference for each lead time and dashed lines indicate +/- one standard deviations
326 around the mean for the samples at a given lead time, averaged over all of the low, medium,
327 and high-priority cases.

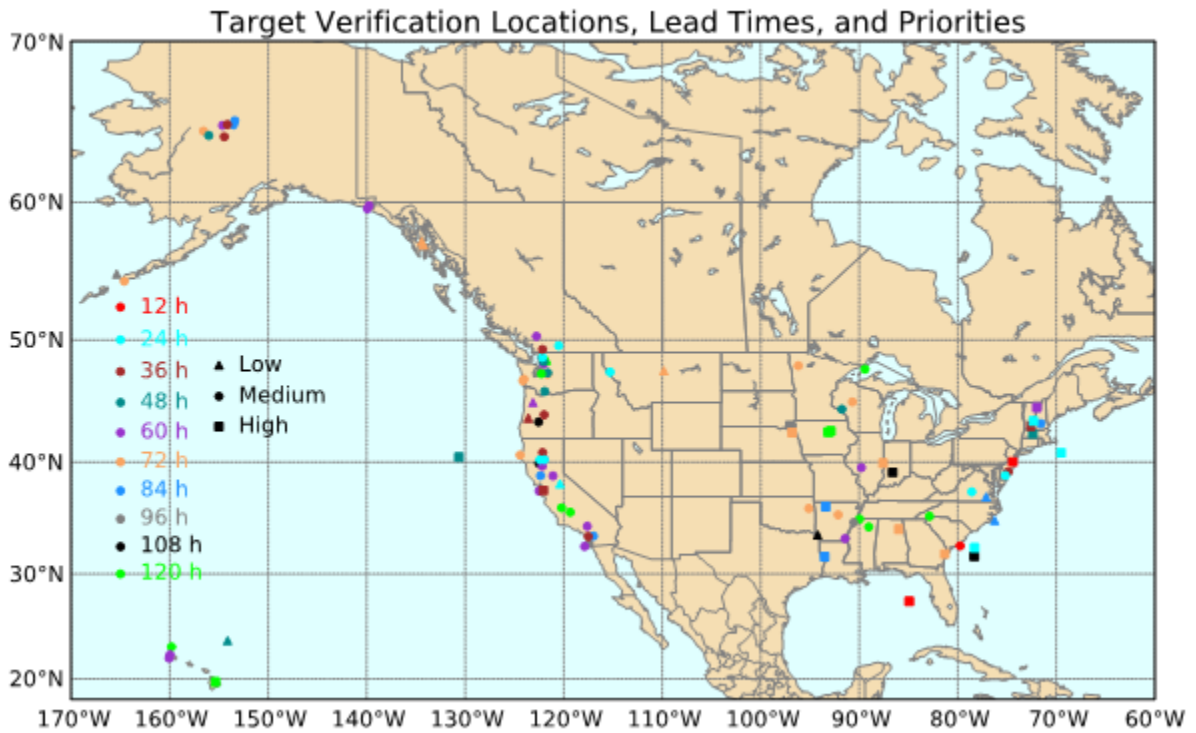
328 **Figure 3:** As in Fig. 2, but for the PNA region (20° N - 75° N, 180° E - 320° E).

329 **Figure 4:** Equitable threat score and bias score for 24-hour accumulated precipitation
330 from forecast hours +24 to +48 verified over the contiguous US. Top panels provide the
331 scores, and bottom panels provide the difference (solid lines) between the NODROP and
332 CONTROL experiments and 95% confidence intervals (bars) based on 1000 realizations of
333 Monte-Carlo tests.

334 **Figure 5:** As in Fig. 4, but for 24-hour accumulated precipitation from forecast hours +48
335 to +72.

336

337



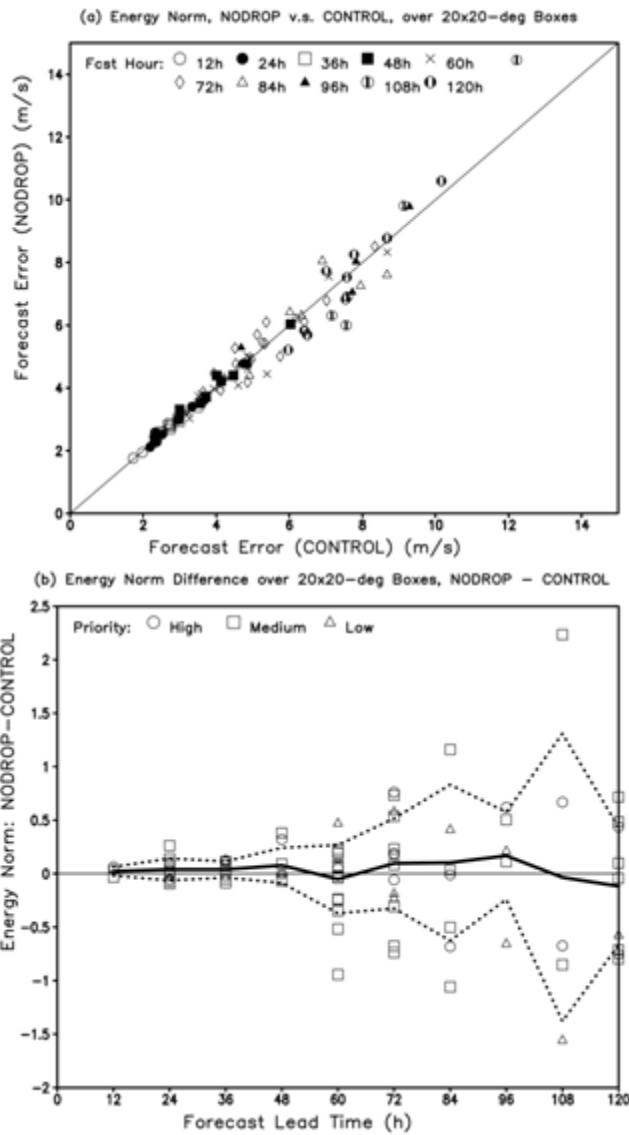
338 **Figure 1:** Scatterplot of the target central locations. Triangles denote low-priority cases, filled
339 circles for medium-priority, squares for high priority. The forecast lead time is denoted by the color
340 of the symbol, indicated by the legend on the left-hand side.

341

342

343

344



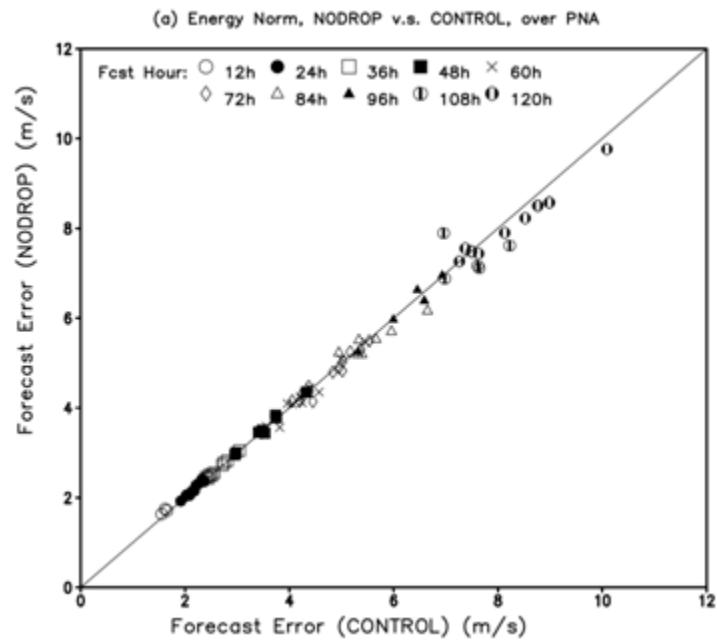
345

346

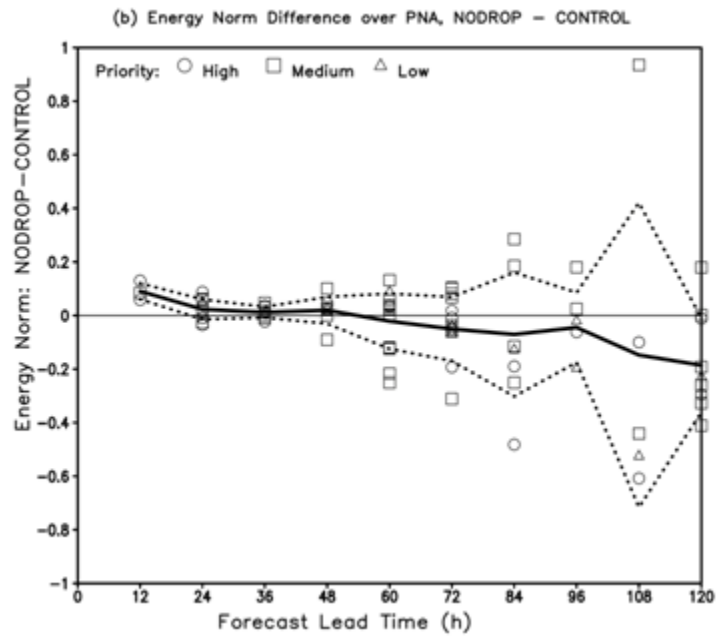
347 **Figure 2.** (a) Scatterplot of forecast errors for the target verification regions, CONTROL (x-axis) vs.
348 NODROP (y-axis). Data for the different forecast lead times are denoted by different symbols, as
349 shown in the figure legend. (b) Differences of the energy norm between the NODROP and CONTROL
350 experiments. Bold line indicates the mean difference for each lead time and dashed lines indicate
351 +/- one standard deviations around the mean for the samples at a given lead time, averaged over all
352 of the low, medium, and high-priority cases.

353

354



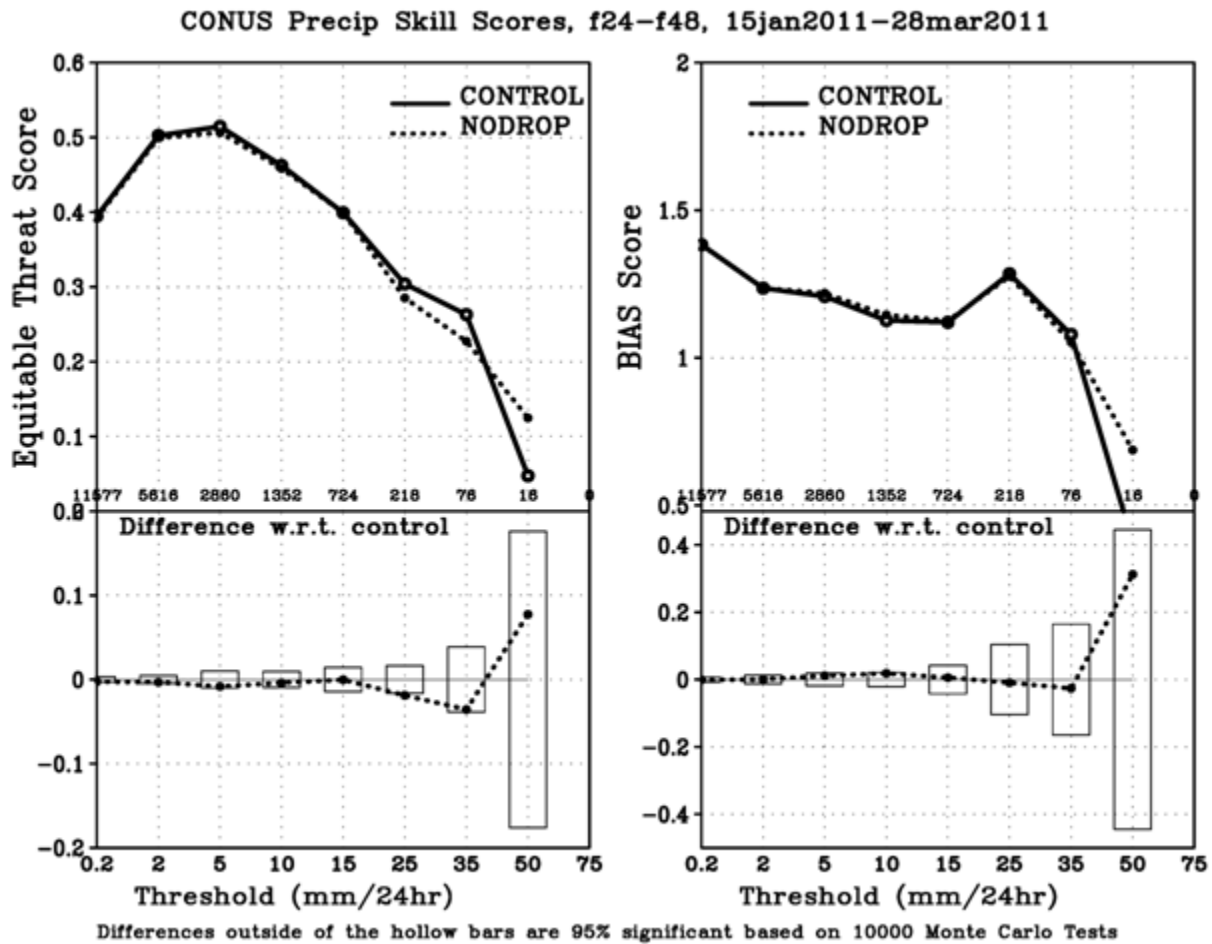
355



356 **Figure 3:** As in Fig. 2, but for the PNA region (20° N - 75° N, 180° E - 320° E).

357

358
359
360



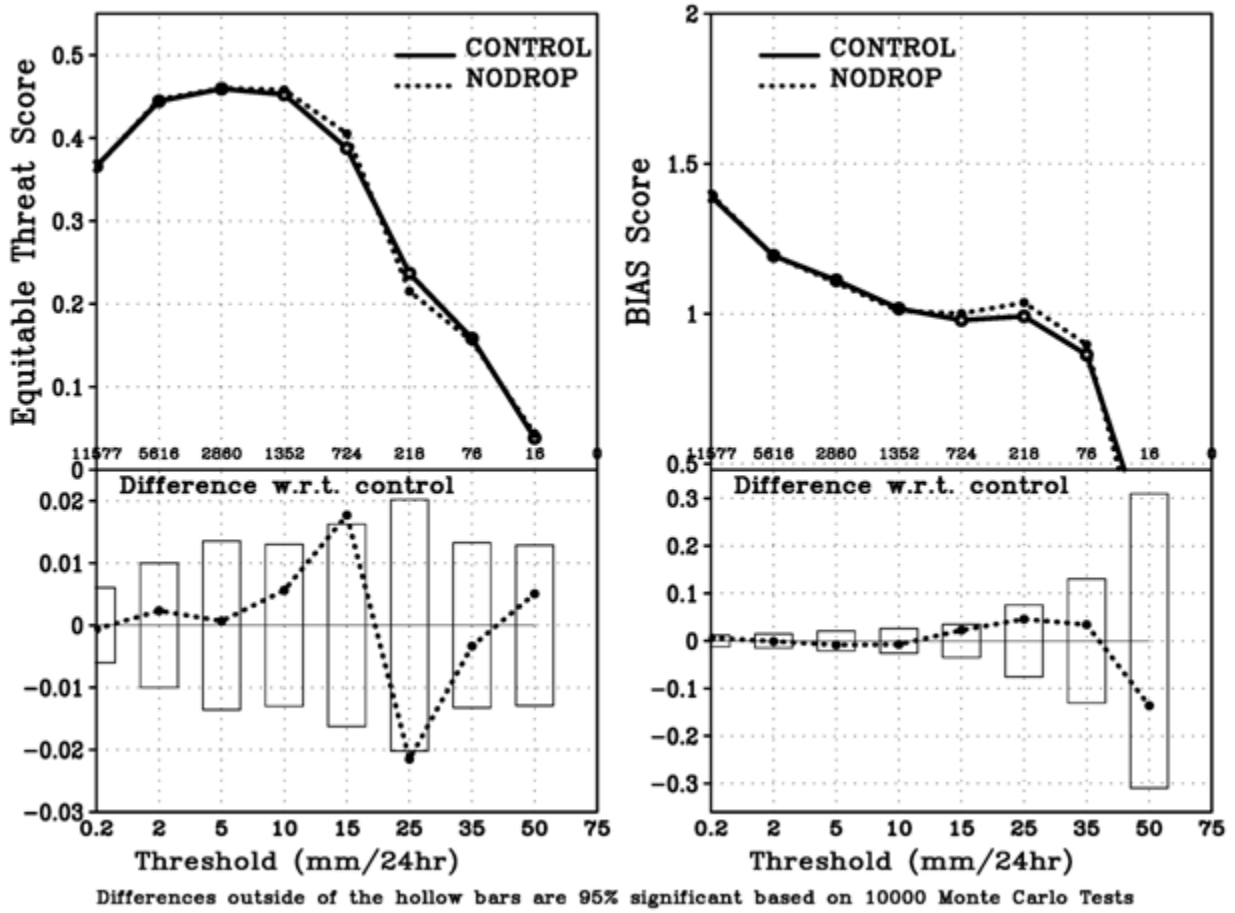
361

362

363 **Figure 4:** Equitable threat score and bias score for 24-hour accumulated precipitation from
364 forecast hours +24 to +48 verified over the contiguous US. Top panels provide the scores, and
365 bottom panels provide the difference (solid lines) between the NODROP and CONTROL
366 experiments and 95% confidence intervals (bars) based on 1000 realizations of Monte-Carlo tests.

367

CONUS Precip Skill Scores, f48-f72, 15jan2011-28mar2011



368

369

370 **Figure 5:** As in Fig. 4, but for 24-hour accumulated precipitation from forecast hours +48 to +72.

371